Journal of Geoscience and Environment Protection, 2026, 14(4), 390-407
https://www.scirp.org/journal/gep
ISSN Online: 2327-4344
ISSN Print: 2327-4336

Research and Application of Prestack Seismic-Geological Interaction Modeling Technology

Lei Du[1,2], Guofa Li[1], Xiaoguang Li[3], Sifan Zhan[4], Desheng Dong[2], Chenyang Gao[2]

[1]College of Geophysics, China University of Petroleum (Beijing), Beijing, China
[2]Research Institute of Petroleum Exploration and Development, PetroChina Liaohe Oilfield Company, Panjin, China
[3]PetroChina Liaohe Oilfield Company, Panjin, China
[4]Bureau of Geophysical Prospecting Inc., PetroChina, Zhuozhou, China
Email: dulei0319@163.com

How to cite this paper: Du, L., Li, G. F., Li, X. G., Zhan, S. F., Dong, D. S., & Gao, C. Y. (2026). Research and Application of Prestack Seismic-Geological Interaction Modeling Technology. *Journal of Geoscience and Environment Protection, 14,* 390-407.
https://doi.org/10.4236/gep.2026.144021

Received: December 7, 2025
Accepted: April 27, 2026
Published: April 30, 2026

Abstract

In order to solve the problem of thin reservoir prediction in the context of horizontal well development, a prestack seismic-geological modeling technology suitable for the characteristics of shale oil in Liaohe Depression was studied and summarized. This technology makes full use of the "two widespread and one high" seismic data, seismic interpretation results, velocity data and prestack inversion results to establish high-precision models, so that the seismic information plays a leading role in the modeling process and improves the model's lateral accuracy. The research results show that seismic-geological interaction modeling under prestack seismic prediction constraints can greatly improve the vertical and horizontal resolution of the model, provide a basis for the optimization of horizontal well trajectory and dynamic adjustment, improve the drilling rate of horizontal wells, and meet the exploration deployment and horizontal well drilling needs of the Shale oil reservoir in the middle of the Damintun sag of Liaohe.

Keywords

Shale Oil, Seismic-Geology, Velocity Modeling, Well-Seismic Interactive Modeling, Lateral Resolution

1. Introduction

In the 1980s, stochastic simulation techniques emerged to address various geological and engineering challenges encountered throughout hydrocarbon exploration and development (Haas & Dubrule, 1994; Mosegaard & Tarantola, 1995; Francis,

2006a, 2006b; Zhang et al., 2012; Wu, Fu, & Lan, 2008). Guardiano and Srivastava (1993) pioneered the introduction of multiple-point geostatistics into the field of stochastic modeling. Subsequently, the SNESIM (Single Normal Equation Simulation) algorithm proposed by Strebelle and Journel (2001) established a crucial foundation for the practical application of multiple-point geostatistics in reservoir modeling.

Chinese scholars have also conducted in-depth research in this domain. Yin, Wu, Zhang et al. (2008) proposed a reservoir framework-based multiple-point geostatistical modeling method, demonstrating its enhanced effectiveness in characterizing the spatial architecture of fluvial facies reservoirs. Yin, Zhang, & Li (2014) further advanced a depositional pattern-based multiple-point geostatistical approach, which effectively mitigated simulation biases inherent in modeling non-stationary reservoirs. Feng, Wu, Yin et al. (2014) developed a Vector-based Multiple-Point Statistics (VMPS) algorithm that integrates geological vector information, validating its adaptability under strongly non-stationary conditions through both conceptual models and actual reservoir case studies. Wang and Duan (2023) addressed the weak integration of geological significance in traditional multiple-point geostatistical modeling by introducing a facies-sequence constrained multiple-point geostatistical facies modeling technique, which significantly improved the representation of spatial distribution patterns for different sedimentary facies.

Beyond theoretical and methodological explorations, domestic researchers have extensively applied multiple-point geostatistical modeling techniques to various reservoir types, conducting widespread application studies (e.g., Feng, Chen, Zhang et al., 2005; Zhou, Gui, Li et al., 2010; Lyu, Li et al., 2024). These practical applications have effectively enhanced the consistency between the constructed geological models and actual drilling data, thereby meeting, to a certain extent, the urgent demand for high-precision reservoir models during the oilfield production stage.

On the Integration of Seismic and Well Log Data in Geological Modeling, Araktingi & Bashore (1992) systematically elaborated on methodologies and workflows for integrating seismic and well log data to model reservoir property parameters. Wu, Zhang, Li et al. (2001) summarized fundamental geological constraints to be adhered to during modeling and, based on these, proposed a stochastically geological modeling framework under geological constraints, detailing its conceptual approach and implementation. Yin, Liu et al. (2002) reviewed techniques and advances in integrating seismic data into geological models. Mu, Zhou, Zhang et al. (2009) applied resistivity pseudo-acoustic inversion technology, combining qualitative and quantitative analysis within a geology-logging-seismic integration framework to predict sandstone reservoir distribution, thereby enhancing hydrocarbon detection accuracy. Jia, Xu, Chen et al. (2010) developed an integrated well-seismic modeling approach suitable for thin sand-shale interbeds by directly combining seismic attributes, seismic inversion data, and well log information. Chen, Zhao, Cao et al. (2014) systematically compared the

advantages and limitations of variogram-based, facies-controlled, and seismic-attribute-constrained modeling methods, highlighting the necessity of multi-information integration in reservoir modeling. Jia (2021) utilized geostatistical inversion results as trend constraints to construct a facies model, effectively capturing the spatial distribution characteristics of sand bodies.

However, these conventional modeling methods remain predominantly well-centric. Although some approaches incorporate multiple constraints, their reliability is largely confined to well locations, while inter-well predictions rely on stochastic mathematical algorithms. As the distance from well points increases, the consistency between modeling results and geological understanding diminishes. Existing methodologies are inadequate to meet the requirements for high-precision geological models in shale oil reservoirs with long horizontal well sections. Therefore, this study proposes a novel seismic-geological integrated modeling methodology driven primarily by seismic data.

The pre-stack seismic-geological modeling workflow begins by converting time-domain seismic interpretation results and pre-stack inversion volumes to the depth domain using a high-precision velocity field, thereby constructing a 3D depth-domain velocity model. This ensures that seismic information exerts a dominant constraining role throughout the modeling process. Subsequently, a structural framework model is built based on 3D seismic interpretation data and calibrated with well stratification, significantly enhancing the lateral prediction accuracy of the structural model. This enables reliable support for horizontal well trajectory design and real-time geosteering. Finally, lithology and reservoir attribute modeling are conducted by integrating elastic parameter volumes derived from "wide-azimuth, wide-frequency, and high-density" pre-stack seismic inversion as spatial constraints. This approach not only preserves the vertical resolution of the model but also substantially improves the reliability of lateral property predictions. The results can be directly applied to fine-tuning horizontal well trajectories, real-time drilling analysis, and geosteering decisions.

The Damintun Sag, a first-order tectonic unit in the northeastern Liaohe Basin within the Bohai Bay Rift System, is bounded by faults and is recognized as a typical "small but prolific" oil-bearing depression in eastern China. During the early depositional stage of the Sha-4 Member of the Shahejie Formation, a sedimentary sequence dominated by carbonate-rich oil shales interbedded with argillaceous dolomites developed in the central part of the sag, making it a favorable target for shale oil exploration. However, the shale oil reservoirs are characterized by thin single layers, diverse storage spaces, and complex mineral compositions. Early seismic models constructed using conventional methods suffered from low accuracy, leading to significant uncertainties in predicting "geological sweet spots" (e.g., zones with high organic matter content, high brittleness, and developed fractures). Consequently, drilling often failed to accurately penetrate high-quality reservoirs, directly impeding the optimization of horizontal well placement and the design of subsequent hydraulic fracturing operations.

2. Initial Geological Model for Shale Oil

2.1. Velocity Modeling and Time-Depth Conversion

Based on the precise time-depth relationship derived from single-well velocity analysis, a high-precision 3D velocity field was constructed by extrapolating well-based velocities and performing 3D spatial interpolation, constrained by seismically interpreted horizons and a structural framework model (**Figure 1**). This velocity field effectively integrates the high vertical resolution of logging data with the extensive lateral coverage of seismic data, significantly enhancing the accuracy of the spatial velocity model. Subsequently, this 3D velocity model was applied to convert time-domain seismic horizons, fault interpretations, and pre-stack inversion volumes to the depth domain, generating depth-structural and attribute models. These outputs provide a reliable depth-domain foundation for detailed reservoir characterization and well trajectory design.

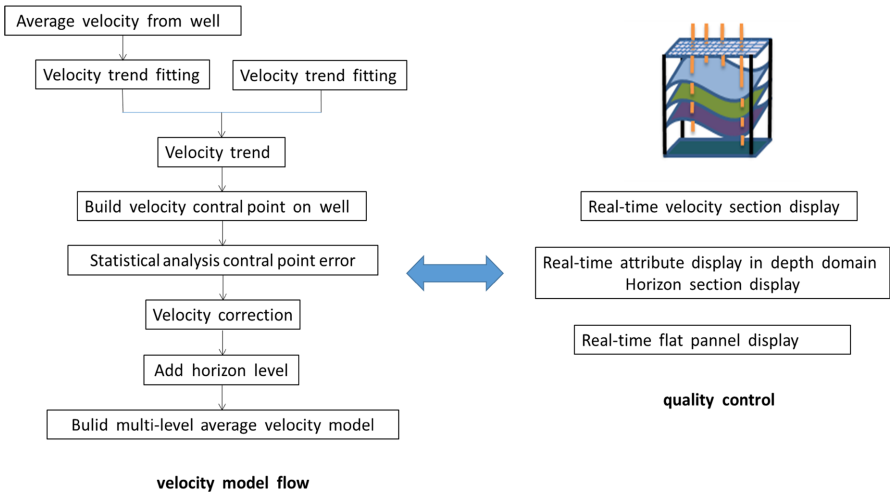

Figure 1. Velocity modeling flow diagram.

2.2. Fault Surface and Horizon Modeling

Fault Surface Modeling: based on seismically interpreted fault point sets or fault surface data, a spatial interpolation algorithm is employed to construct an initial fault surface grid model. This workflow automatically generates the geometric morphology of the fault surface, including the definition of fault boundaries and the calculation of grid dimensions. The automatically generated surfaces are subsequently edited, including the optimization of fault line data, adjustment of fault boundaries, and smoothing of the surfaces. Fault line editing primarily involves the removal and correction of outliers or redundant portions in the interpreted data, thereby refining the geometric shape of the fault boundaries. This process ensures that the final constructed fault surfaces are not only consistent with the original data constraints but also exhibit geologically reasonable geometries.

Fault Contact Relationship Processing: to address the discontinuities between interpreted fault surfaces, the contact relationships between faults are processed

in an integrated manner to achieve seamless cutting of fault surfaces. The modeling software automatically identifies primary and secondary faults based on geometric topological relationships and generates vector connection lines from the secondary fault to the primary fault along the tangential direction. These vector lines can be interactively edited and are ultimately used to fill the gaps between primary and secondary faults. If a secondary fault extends beyond the primary fault, the overhanging portion is automatically truncated to maintain the spatial consistency of the fault system.

Horizon Modeling and Fault Integration: based on the fault surface model, horizon data are used to construct an initial horizon model. At this stage, the model does not incorporate fault constraints. The horizon data can be edited, including correction of interpreted data, optimization of horizon boundaries, and grid refinement. The fault surfaces are used to cut the horizon model, and the intersection lines between them are calculated. These intersection lines are edited to eliminate spatial conflicts. The horizons are then split along the intersection lines, and the vertical and horizontal fault throws are calculated. During this process, conflicting or non-closing points along the fault lines can be interactively removed, ultimately resulting in a high-precision, fault-controlled horizon model.

Well Marker Calibration and Model Output: well marker data are used to further calibrate the horizon model, ensuring that the modeled horizons accurately match the well markers. This yields a well-controlled optimized structural model (**Figure 2**). This study established structural models for four horizons: the top of Sand Group I, top of Sand Group II, top of Sand Group III, and the base of Sand Group III, providing a reliable structural framework for subsequent reservoir prediction and well trajectory design.

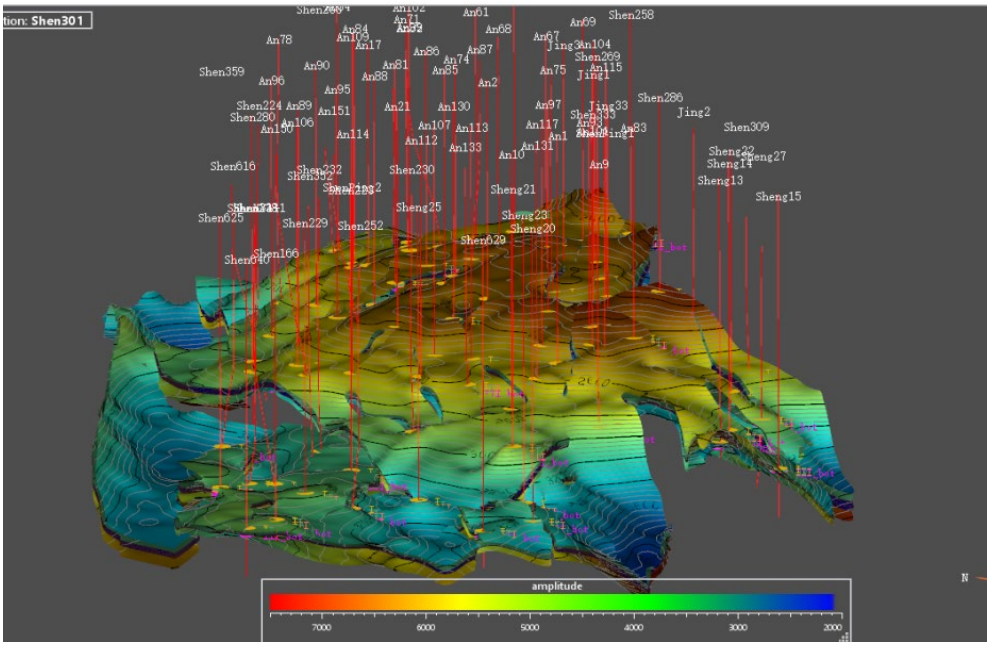

Figure 2. Fine structural model after well stratification correction.

2.3. Reservoir Grid Modeling

A three-dimensional reservoir geocellular model was constructed based on the structural framework defined by four key horizons: the top of Sand Group I, top of Sand Group II, top of Sand Group III, and base of Sand Group III. The model employs a regular hexahedral grid configuration with a horizontal spacing of 30 m × 30 m and a vertical resolution of 1 m, maintaining conformable parallel contacts between successive strata.

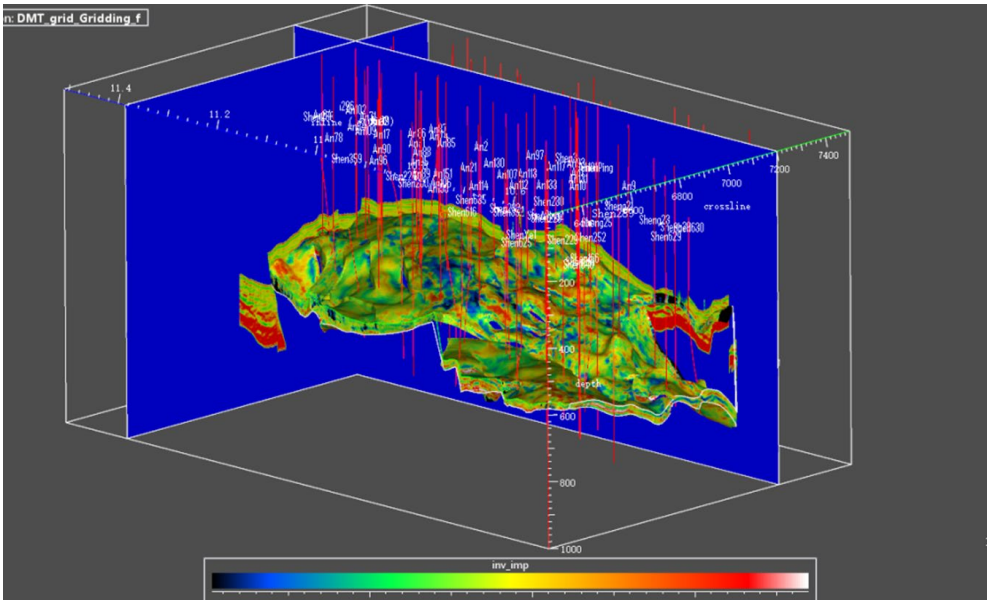

Figure 3. Three-dimensional wave impedance attribute volume.

Property modeling was implemented within this geological grid system, utilizing pre-stack seismic inversion results as soft constraints for both facies and reservoir parameter modeling. The workflow involved loading depth-converted seismic volumes and resampling pre-stack inversion-derived attributes—including P-impedance, S-impedance, and Poisson's ratio—into the geological grid space. This process generated a P-impedance attribute volume and corresponding reservoir grid model (**Figure 3**).

For facies modeling, the integration of P-impedance, S-impedance and Poisson's ratio as cooperative constraints enabled the full utilization of "wide-azimuth, wide-bandwidth, and high-density" seismic data in guiding spatial characterization. The resulting high-resolution attribute model provides reliable geological support for optimized horizontal well placement and drilling operations in the study area.

3. Property Modeling

3.1. Approaches and Fundamentals of Modeling

Lithofacies modeling serves as the foundation for reservoir property modeling, focusing on predicting the spatial distribution of discrete lithofacies types through stochastic simulation methods. Current stochastic modeling approaches are pri-

marily divided into two categories: Object-Based Modeling and Pixel-Based Sequential Simulation. Object-Based Modeling employs an object-based stochastic placement algorithm, suitable for geological bodies with distinct geometric shapes (such as channels or deltas). However, the simulation results exhibit significant uncertainty (strong multiplicity of solutions) and struggle to effectively incorporate seismic attributes as spatial constraints. Consequently, this method is less suitable for shale oil reservoirs that demand high modeling precision.

Pixel-Based Sequential Simulation methods mainly include Sequential Indicator Simulation (SIS) and Truncated Gaussian Simulation (TGS). Both methods offer high vertical resolution and can effectively integrate seismic attributes as soft constraint data. Nevertheless, SIS results often suffer from insufficient lateral continuity. Therefore, this study adopts the TGS algorithm for lithofacies modeling.

The fundamental difference between TGS and indicator simulation lies in its treatment of discrete lithofacies as realizations of a continuous variable: a continuous random field is first generated using Sequential Gaussian Simulation. Then, based on the cumulative probability distribution functions of different lithofacies, truncation thresholds are set to convert the continuous variable into a discrete lithofacies model. This study uses lithofacies interpretation data from well points as hard data to establish the initial lithofacies model using the TGS method.

To further enhance model accuracy, pre-stack seismic inversion results—namely P-impedance, S-impedance, and Poisson's ratio—are introduced as co-constraining variables. Lithofacies modeling is performed using a multi-attribute co-simulation algorithm.

Co-simulation is essentially a Gaussian simulation method based on the Co-Kriging framework. Its algorithmic principle can be described as follows:

The theoretical foundation of Kriging relies on the second-order stationarity assumption of random variables, which requires the mathematical expectation of a random variable to be constant across space. However, this assumption can lead to multi-solution issues in estimates at locations far from control points. To address this, it is necessary to characterize the spatial variation of the expectation function m(x). Drift Kriging (e.g., Universal Kriging) achieves this by estimating m(x) from sample data.

Seismic data provide a reliable basis for estimating m(x). For example, 3D seismic volumes or acoustic impedance data can be used to derive m(x). Alternatively, the Co-Kriging algorithm incorporates seismic data as "soft data" to impose macroscopic constraints. This approach effectively integrates multiple information sources, leveraging the high vertical resolution of well data and the lateral continuity of seismic data, thereby significantly improving estimation accuracy.

Ordinary Kriging primarily addresses univariate estimation. In practice, data often involve multiple variables. Besides the primary variable (e.g., reservoir properties), one or more secondary variables (e.g., seismic impedance, amplitude) may exhibit spatial cross-correlation with the primary variable, containing valuable in-

formation for estimation. Co-Kriging was developed to incorporate these variables comprehensively.

Co-Kriging enhances estimation precision by leveraging spatial correlations among multiple variables. In reservoir characterization, where well data are often sparse horizontally, integrating seismic data as a macroscopic constraint through Co-Kriging can notably improve results.

Assume n primary variables (hard data):

$$Z\left(\mu_\alpha\right), i=1,\cdots,n$$

and N secondary variables (soft data):

$$y\left(\mu_i\right), j=1,\cdots,N$$

The Co-Kriging estimate at any point is expressed as a linear combination:

$$Z_0^* = \sum_{i=1}^{n} \alpha_i Z_i + \sum_{j=1}^{N} \beta_j y_j \tag{1}$$

where Z_0^* is the estimated value of Z at location 0, $\alpha_1,\cdots,\alpha_n$ and $\beta_1,\cdots,\beta_N$ are Co-Kriging weights to be determined. This requires incorporating correlation coefficients between primary and secondary variables.

For Simple Co-Kriging (SCK), regionalized variables are assumed second-order stationary, with a known constant expectation $E\left[Z\left(x\right)\right]=m_Z$. The variables are centered by defining $Z^*\left(\mu\right)=Z\left(\mu\right)-m_Z$, leading to the SCK estimate:

$$Z^*\left(\mu\right)-m_z = \sum_{i=1}^{n} \alpha_i \left[Z\left(\mu_\alpha - m_z\right)\right] + \sum_{j=1}^{N} \beta_j \left[y\left(\mu_i - m_Y\right)\right] \tag{2}$$

where m_z is the expectation of the primary variable, and m_Y is the expectation of the secondary variable.

The estimation variance is given by:

$$\sigma^2\left(u\right) = C_z\left(0\right) - \sum_{i=1}^{n} \alpha_i C_z\left(\mu_\alpha - \mu\right) - \sum_{j=1}^{N} \beta_j C_{zy}\left(\mu_i - \mu\right) \tag{3}$$

Using the least squares principle, the SCK system of equations is derived:

$$\begin{cases} \sum_{i=1}^{n} \alpha_i C_z\left(\mu_\alpha - \mu_\beta\right) + \sum_{j=1}^{N} \beta_j C_{zy}\left(\mu_\alpha - \mu_j\right) = C_z\left(\mu_\alpha - \mu\right) & \alpha = 1,\cdots,n \\ \sum_{i=1}^{n} \alpha_i C_{zy}\left(\mu_i - \mu_\beta\right) + \sum_{j=1}^{N} \beta_j C_y\left(\mu_i - \mu_j\right) = C_z\left(\mu_i - \mu\right) & i = 1,\cdots,n \end{cases} \tag{4}$$

This (n+N)-dimensional system solves for weights $\lambda_\beta(\mu)$ and $\lambda_j(\mu)$. Key covariance functions include:

$C_Z\left(h\right)$: covariance of the primary variable Z;

$C_Y\left(h\right)$: covariance of the secondary variable Y;

$C_{ZY}\left(h\right)$: cross-covariance between Z and Y.

Despite its theoretical advantages, Co-Kriging has limitations: the covariance matrix is complex, and screening effects may occur where data strongly correlated with the estimation point (e.g., primary samples) dominate over weakly correlated data (e.g., secondary variables), potentially biasing results. These issues limit prac-

tical application, leading to preferences for External Drift Kriging or Collocated Co-Kriging.

Collocated Co-Kriging is a simplified form of Co-Kriging. When secondary variables (e.g., seismic attributes) are densely sampled, it retains only the secondary variable value at the estimation location, ignoring other secondary samples. This is particularly useful for seismic soft constraints, as seismic data provide continuous coverage at every grid node.

The estimate is expressed as:

$$Z^*(\mu)=\sum_{i=1}^{n}\lambda_i Z(\mu_\alpha)+\lambda_s y(\mu) \tag{5}$$

where $Z^*(\mu)$ is the estimate at u, $Z(\mu_\alpha)$ are primary samples, $y(u)$ is the collocated secondary value, λ_i and λ_s are weights. The corresponding system is:

$$\begin{cases}\sum_{\beta=1}^{n}\lambda_\beta C_z(\mu_\alpha-\mu_\beta)+\lambda_s C_{zy}(\mu_\alpha-\mu)=C_z(\mu_\alpha-\mu) & \alpha=1,\cdots,n\\ \sum_{\beta=1}^{n}\lambda_\beta C_{zy}(\mu_\beta-\mu)+\lambda_s C_y(0)=C_{yz}(0)\end{cases} \tag{6}$$

This requires modeling $C_Z(h)$, $C_Y(h)$, and $C_{ZY}(h)$. The cross-covariance $C_{ZY}(h)$ can be approximated as:

$$C_{zy}(h)=\beta\cdot C_z(h) \tag{7}$$

where:

$$\beta=p_{zy}(0)\sqrt{\frac{C_y(0)}{C_z(0)}} \tag{8}$$

where $C_Z(0)$ and $C_Y(0)$ are the variances (sills) of Z and Y at zero lag, and $p_{ZY}(0)$ is the linear correlation coefficient at the collocated location. This approximation simplifies cross-covariance modeling.

3.2. Workflow and Outcomes of Modeling

To enhance the accuracy and reliability of lithofacies modeling, this study utilizes pre-stack seismic inversion results as spatial constraints and integrates borehole lithology data with seismic wave impedance attributes for co-simulation. The specific workflow and methodology are as follows.

3.2.1. Data Integration and Correlation Analysis

First, cross-plot analysis between wave impedance and lithology confirms a positive correlation between the two. However, the correlation coefficient is 0.61, indicating that the seismic attribute has a limited direct discriminative capability for lithology. Given this context, a co-simulation method is adopted. Lithology data from 93 wells serve as "hard data", and the seismic wave impedance inversion volume acts as "soft data". A joint probability model is constructed by quantifying the correlation between them.

3.2.2. Variogram Analysis and Parameter Optimization

Based on the geological characteristics of the study area, variogram analysis is performed using data from 93 wells and the reservoir grid model. A modeling strategy employing a two-dimensional (2D) horizontal variogram combined with a one-dimensional (1D) vertical variogram is implemented. The vertical range is set to 2 meters to match the vertical resolution requirements of the thin interbedded reservoirs. The principal horizontal ranges are determined through four-direction analysis: the major range is 8600 meters, and the minor range is 6700 meters, reflecting the anisotropic characteristics of the sand body distribution. This parameter setup aims to balance vertical resolution with horizontal continuity.

3.2.3. Co-Simulation Implementation and Result Validation

A 3D lithofacies volume is generated using a co-simulation algorithm. Comparing the connected well profile of wells Shen 280 - Shen 224 - Shen 359 (**Figure 4** shows the wave impedance profile, **Figure 5** shows the lithology simulation profile) reveals that the correlation between wave impedance and lithology is weak (correlation coefficient 0.61), resulting in limited constraint effectiveness from the seismic data. However, the 94 wells in the study area are evenly distributed, and the large horizontal range means the interwell interpolation is primarily constrained by the high-density well control. Thus, the simulation results reliably reflect the spatial trends of lithofacies. A further comparison between unconstrained simulation results and those constrained by pre-stack multi-attributes (**Figure 6**) shows a significant resolution improvement in the constrained model along the horizontal trajectory of well Shenye 1, making it more consistent with sedimentary patterns.

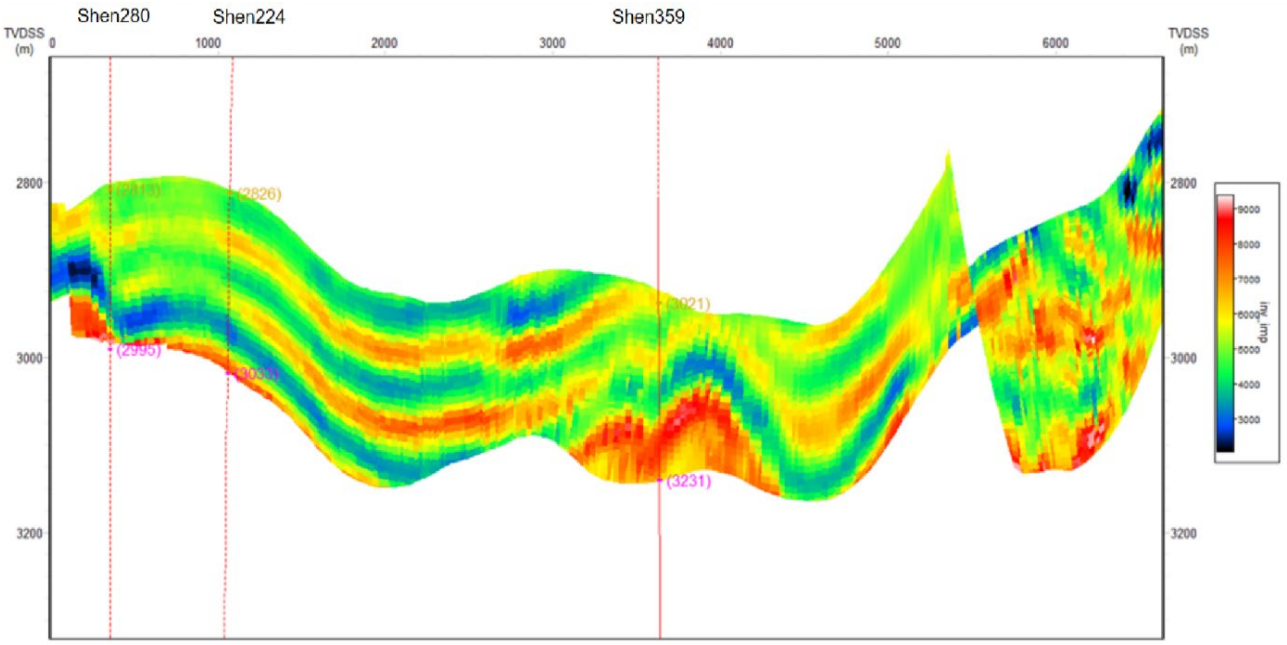

Figure 4. Shen280-Shen224-Shen359 wave impedance profile.

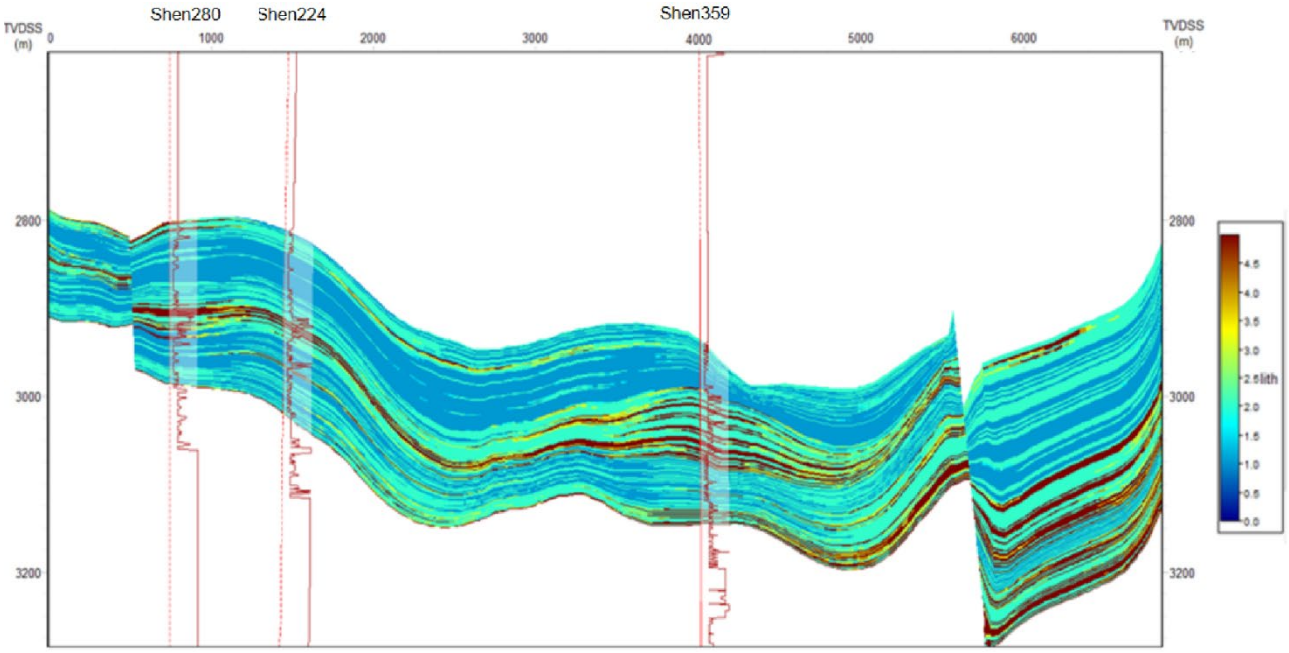

Figure 5. Shen280-Shen224-Shen359 lithology simulation profile.

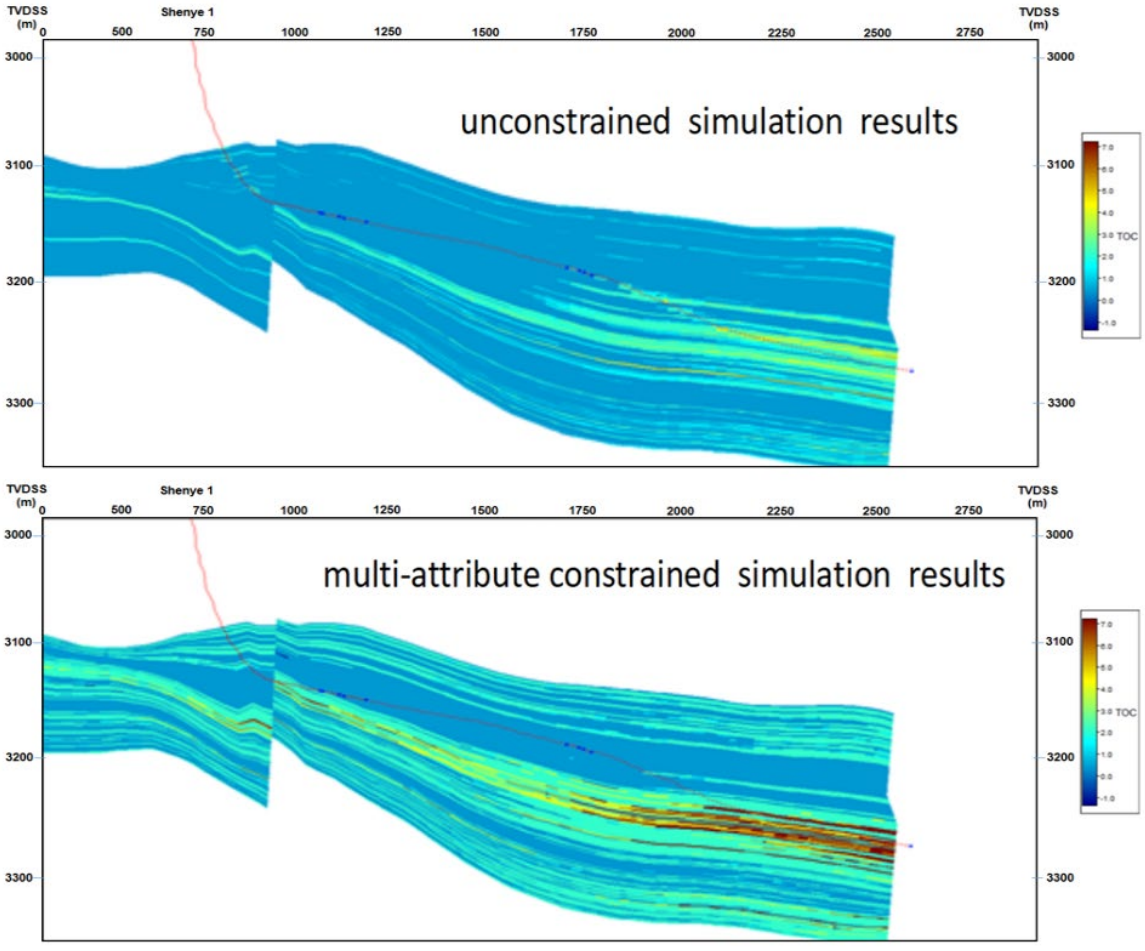

Figure 6. Comparison chart of unconstrained and pre-stack constrained simulated lithofacies along the trajectory of Well Shenye 1.

3.2.4. Effectiveness Evaluation of Seismic Constraints

Cross-plot analysis of measured data from well Shenye 1 and the simulation results (**Figure 7** and **Figure 8**) demonstrates that although the direct correlation coefficient of the pre-stack seismic constraints is not high, these constraints effectively compensate for the lack of information between wells, especially in the horizontal section away from vertical well points, thereby improving lateral prediction accuracy. This highlights the supplementary value of seismic constraints in reducing spatial uncertainty.

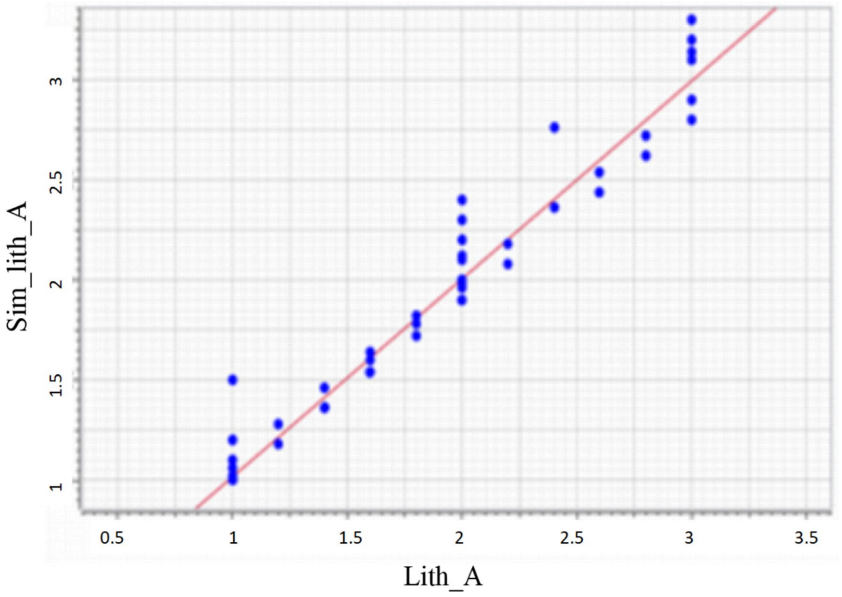

Figure 7. Crossplot of unconstrained simulated lithofacies and well measurement results of Well Shenye 1.

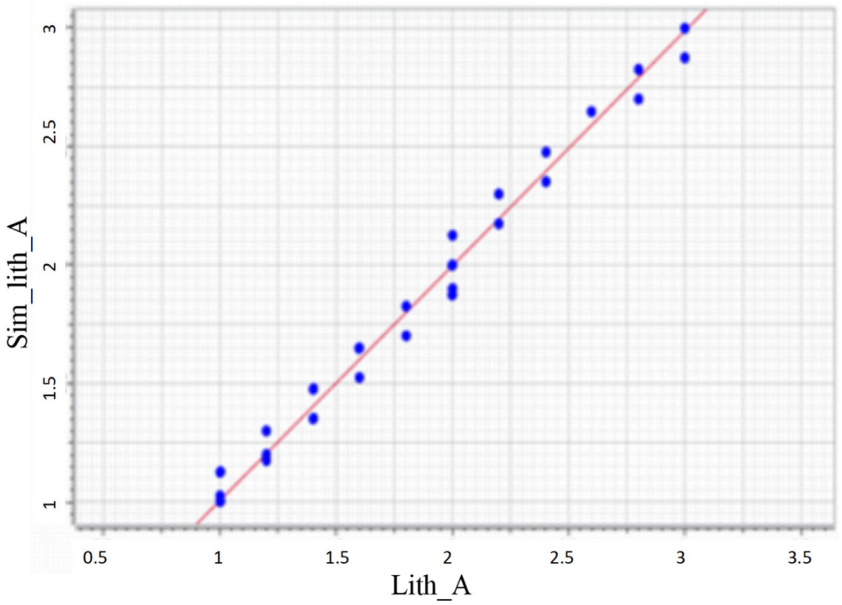

Figure 8. Crossplot of well-seismic constrained simulated lithofacies and well measurement results of Well Shenye 1.

3.2.5. Extension to Facies-Constrained Property Modeling

Based on the lithofacies model, facies-constrained stochastic simulation methods are sequentially employed to build property models for TOC (Total Organic Carbon), GR (Gamma Ray), and RD (Resistivity). The TOC simulation is based on the statistical distribution characteristics of different lithologies (**Figure 9**): shale has the highest TOC values, followed by mudstone, and calcareous sandstone has the lowest. Differential histogram parameters are set for each lithofacies to ensure the property simulations adhere to geological rules. The TOC profile along wells Shen 280 - Shen 224 - Shen 369 (**Figure 10**) further verifies the rationality of the facies-controlled method.

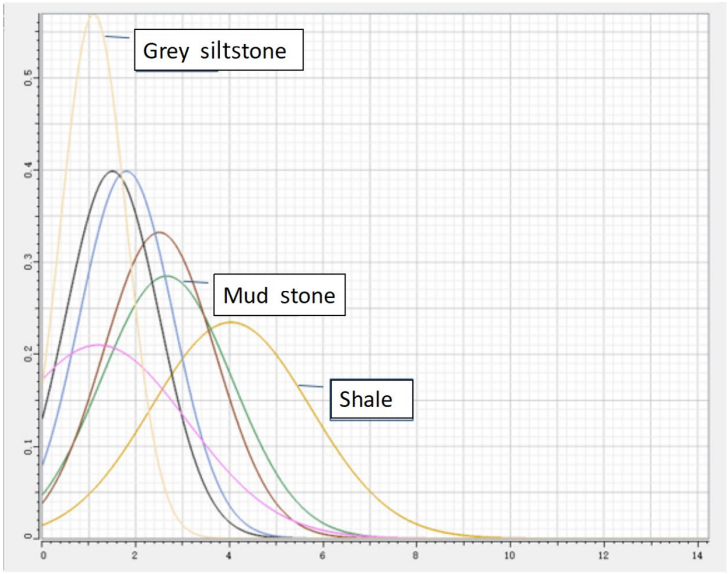

Figure 9. Histogram distribution map of TOC for different lithofacies.

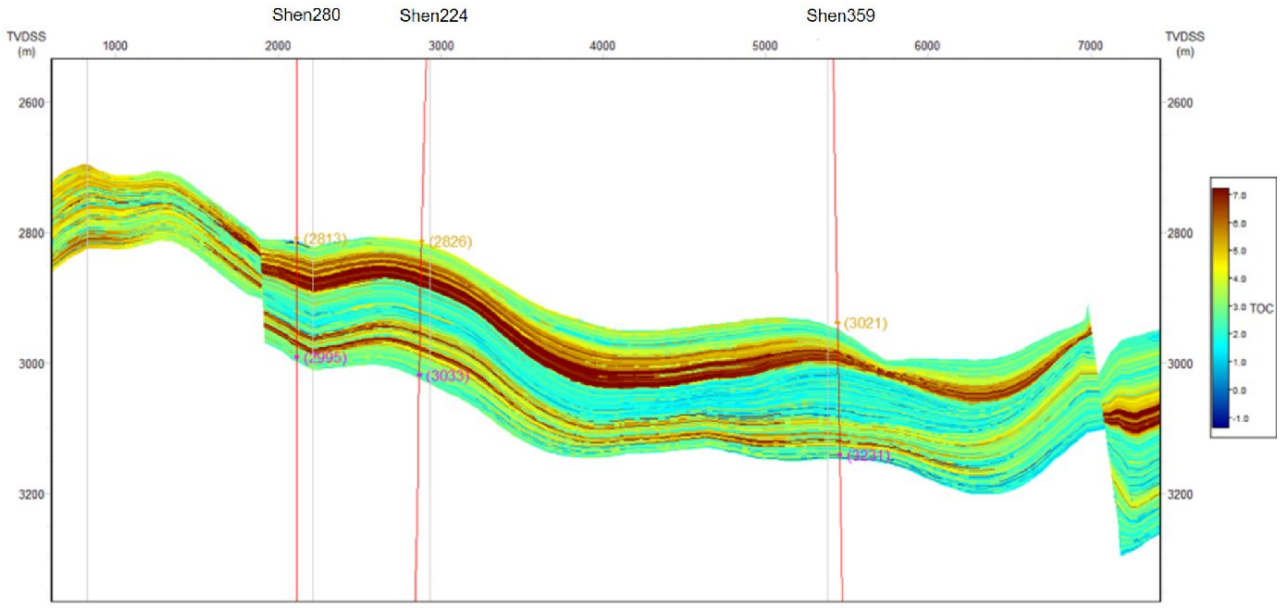

Figure 10. Shen280-Shen224-Shen359 TOC profile.

4. Application of Detailed Geological Models in Real-Time Drilling Analysis

Detailed 3D geological models can effectively support the analysis of the relationship between horizontal well trajectories and formation configuration, real-time geosteering decision-making, and post-drilling evaluation.

Based on structural and attribute volume models, they enable the optimized design of horizontal well drilling plans, real-time geological tracking during the drilling process, and comprehensive post-drilling analysis and model updating. By integrating lithofacies models and key attribute models such as Total Organic Carbon (TOC), the well trajectory can be precisely deployed within "geological-engineering sweet spots", forming a crucial foundation for achieving high drilling encounter rates in shale oil reservoirs and enhancing production capacity.

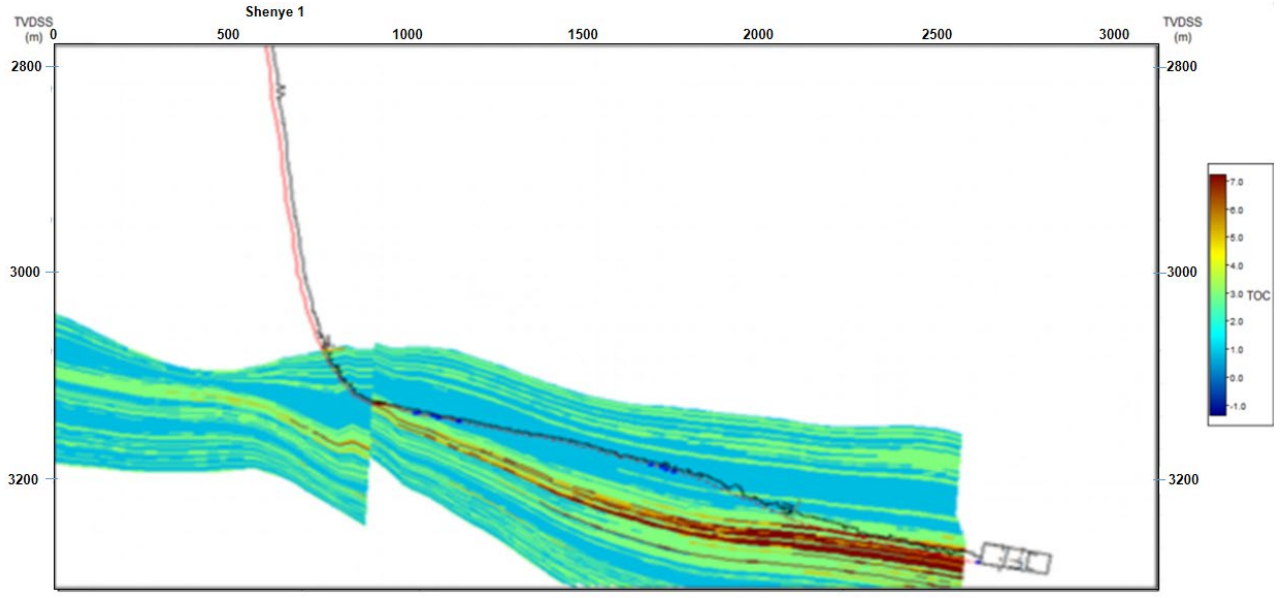

Figure 11. Lithology profile along the trajectory of the horizontal Well Shenye 1.

Figure 11 shows a lithofacies profile along the trajectory of Well Shenye 1, revealing that the well penetrated shale in Sand Group I and dolomite in Sand Group II. Production data indicates that the shale section of Sand Group I contributed the majority of the production. Simulation results suggest that deploying the entire horizontal section within the shale of Sand Group I could potentially yield better production performance.

Among the three horizontal wells deployed in the three-oil-group of the Shen 224 well area within the study area, Well Shen 224-H301 has been completed. Using the actual drilling data from this well to validate the geological model, **Figure 12** displays the lithofacies profile along its trajectory. Model analysis shows that the horizontal section is located in the middle of the interbedded shale layers of the three-oil-group, with the actual drilling trajectory matching the model predictions well, providing excellent geological conditions for subsequent fracturing op-

erations.

Figure 13 presents a 3D visualization of the lithofacies in the Shen 224-H301 well area, showing continuous and stable distribution of shale layers (shown in yellow and dark yellow) along both sides of the horizontal well trajectory. This indicates the potential for long-term stable production after successful fracturing.

Figure 14 shows the TOC attribute profile along the well trajectory, where the model predictions closely match the measured data from drilling samples, demonstrating the high reliability of the model in terms of structural depth and attribute prediction, meeting the requirements for integrated geological-engineering applications.

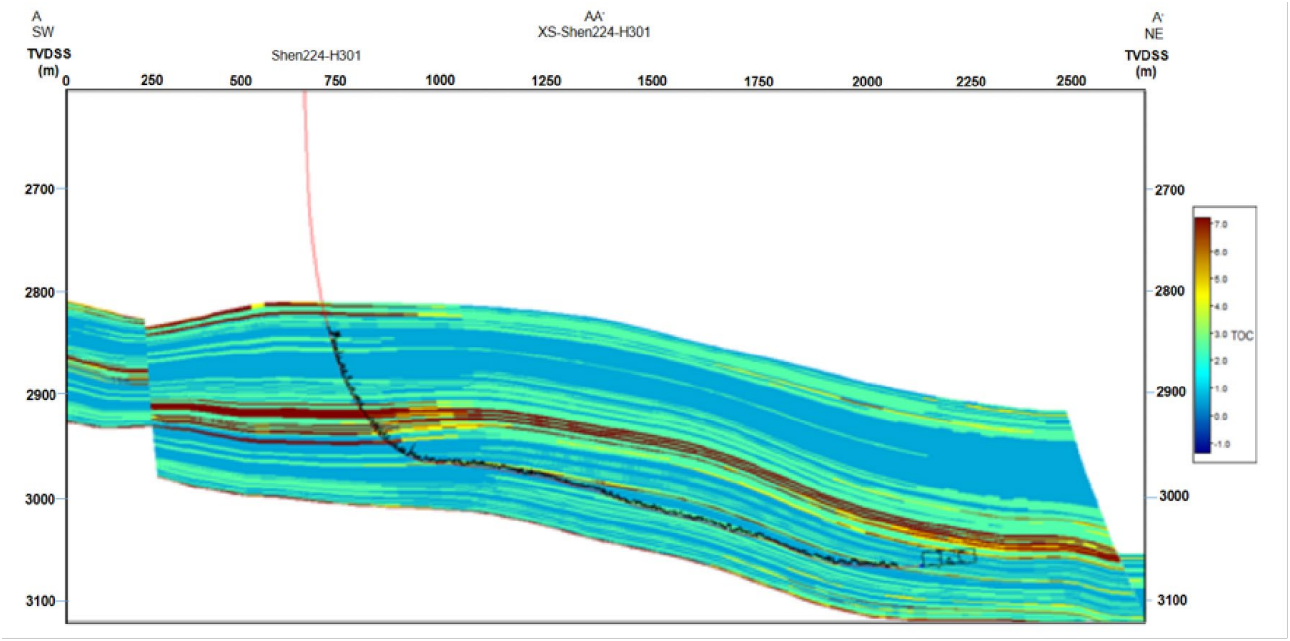

Figure 12. Lithology profile along the trajectory of the horizontal Well Shen 224-H301.

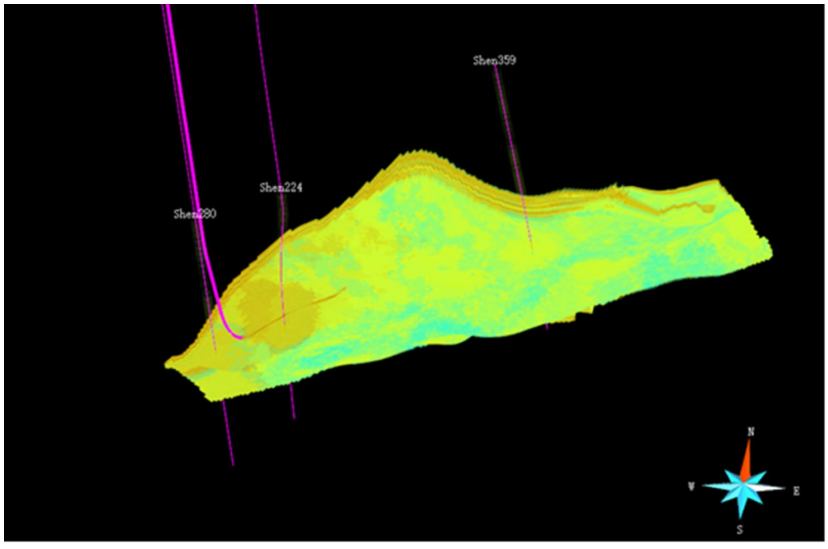

Figure 13. Lithology visualization of Well Shen 224-H301.

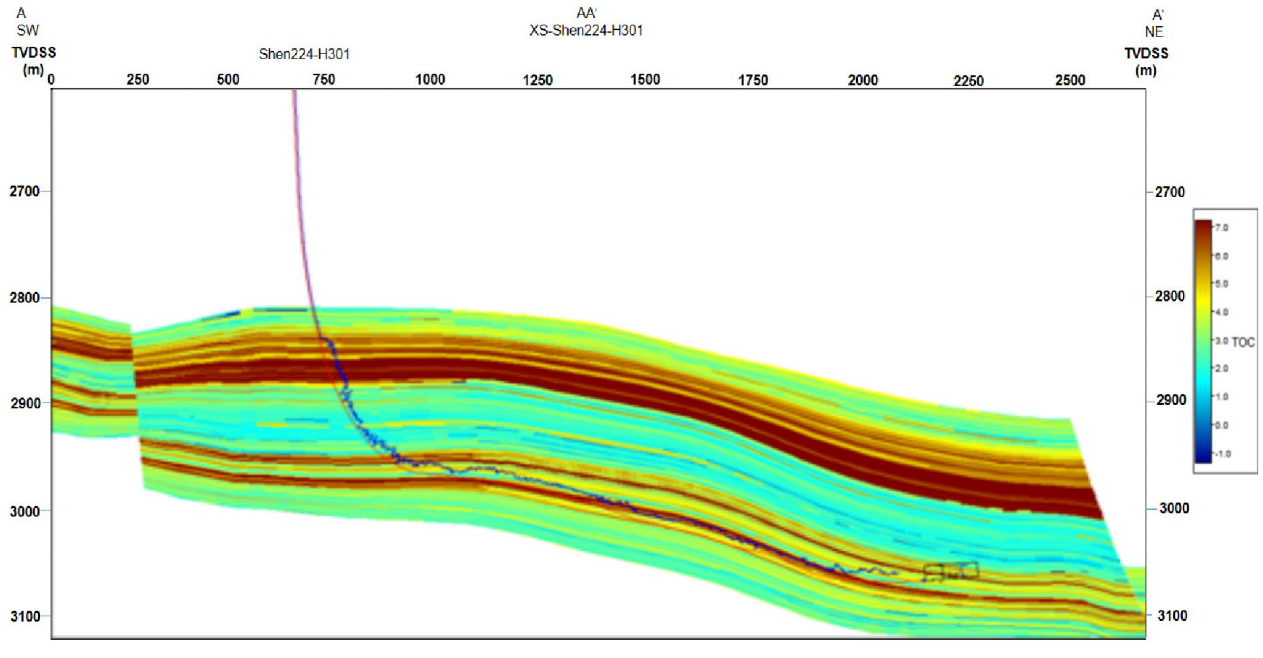

Figure 14. TOC profile along the trajectory of Well Shen 224-H301.

5. Conclusion and Insights

The detailed 3D geological model constructed based on seismic data establishes a seismic-dominant modeling workflow by integrating velocity modeling, structural framework building, lithofacies, and attribute modeling. This model significantly enhances lateral prediction capability while maintaining the vertical resolution of well logs, providing a reliable basis for optimizing horizontal well trajectories and real-time geosteering.

Real-time drilling applications demonstrate that the model effectively supports the analysis of the horizontal well path, real-time geosteering, and post-drilling evaluation. By incorporating lithofacies and geophysical attributes (e.g., TOC) as constraints for dual sweet spot identification, the horizontal section achieves precise placement within high-quality reservoirs, laying a solid geological foundation for enhancing single-well productivity. Validation via well-crossing profiles shows a high consistency between the model-predicted lithofacies distribution and actual drilling results, with a sandstone drill encounter rate exceeding 96%. This confirms the model's reliability in predicting structural depth and attributes, offering effective support for subsequent fracturing operations and production enhancement.

Conflicts of Interest

The authors declare no conflicts of interest regarding the publication of this paper.

References

Araktingi, U. G., & Bashore, W. M. (1992). Effects of Properties in Seismic Data on Res-

ervoir Characterization and Consequent Fluid-Flow Predictions When Integrated with Well Logs. In *SPE Annual Technical Conference and Exhibition* (pp. SPE-24752-MS). SPE. https://doi.org/10.2118/24752-ms

Chen, G. X., Zhao, F., Cao, Z. L. et al. (2014). Integrated Reservoir Modeling Based on Seismic Inversion and Geological Data. *Natural Gas Geoscience, 25,* 1839-1846.

Feng, G. Q., Chen, H., Zhang, L. H. et al. (2005). Stochastic Simulation of Lithofacies Distribution Using Multi-Point Geostatistics. *Journal of Xi'an Shiyou University (Natural Science Edition), 20,* 9-11.

Feng, W. J., Wu, S. H., Yin, S. L. et al. (2014) Avector Information Based Multiple-Point Geostatistic Method. *Journal of Central South University (Science and Technology), 45,* 1261-1268.

Francis, A. M. (2006a). Understanding Stochastic Inversion: Part 1. *First Break, 24,* 69-77. https://doi.org/10.3997/1365-2397.2006026

Francis, A. M. (2006b). Understanding Stochastic Inversion: Part 2. *First Break, 24,* 79-84. https://doi.org/10.3997/1365-2397.2006028

Guardiano, F. B., & Srivastava, R. M. (1993). Multivariate Geostatistics: Beyond Bivariate Moments. In A. Soares (Ed.), *Geostatistics Tróia'92* (pp. 133-144). Springer. https://doi.org/10.1007/978-94-011-1739-5_12

Haas, A., & Dubrule, O. (1994). Geostatistical Inversion—A Sequential Method of Stochastic Reservoir Modelling Constrained by Seismic Data. *First Break, 12,* 564-569. https://doi.org/10.3997/1365-2397.1994034

Jia, T. (2021). *The Application of Reservoir Modeling Technology under 3D Constraint of Seismic Inversion in HC Oilfield of Xinjiang.* China University of Geosciences. https://doi.org/10.27493/d.cnki.gzdzy.2021.001560

Jia, Y. M., Xu, F., Chen, B. et al. (2010). Three-Dimensional Geological Reservoir Modeling of Thin Beds Based on Seismic Data: A Case on Chenghai Oilfield II Area. *Nature Gas Geoscience, 21,* 833-835.

Lyu, X. R., Sun, J. F., Li, H. K. et al. (2024). Fine Geological Modelling Technology for Deep Fractured-Vuggy Carbonate Oil Reservoirs in the Tarim Basin. *Oil & Gas Geology, 45,* 1195-1210.

Mosegaard, K., & Tarantola, A. (1978). Monte Carlo Sampling of Solutions to Inverse Problems. *Journal of Geophysical Research: Solid Earth, 100,* 12431-12447. https://doi.org/10.1029/94jb03097

Mu, Z. Q., Zhou, L. H., Zhang, Y. X. et al. (2009). Application of Seismic-Geologic Integrative Reservoir Prediction Technique in Gu533 Block of Daqing Oilfield. *Oil Geo-Physical Prospecting, 44,* 323-325. https://doi.org/10.13810/j.cnki.issn.1000-7210.2009.03.019

Strebelle, S. B., & Journel, A. G. (2001). Reservoir Modeling Using Multiple-Point Statistics. In *SPE Annual Technical Conference and Exhibition* (pp. SPE-71324-MS). SPE. https://doi.org/10.2118/71324-ms

Wang, M. C., & Duan, T. Z. (2023). Facies Sequence-Based MPS Reservoir Facies Modeling Algorithm and Its Application. *Oil & Gas Geology, 44,* 238-246.

Wu, H. Z., Fu, L. Y., & Lan, Xi. W. (2008). Analysis of Reservoir Heterogeneity Based on Random Media Models. *Progress in Geophysics, 23,* 793-799.

Wu, S. H., Zhang, Y. W., Li, S. J. et al. (2001). Geological Constraint Principles in Reservoir Stochastic Modeling. *Journal of University of Petroleum China (Edition of Nature Science), 25,* 55-58.

Yin, X. Y., & Liu, Y. S. (2002). Methods and Development of Integrating Seismic Data in Reservoir Model-Building. *Oil Geophysical Prospecting, 37,* 423-430.

https://doi.org/10.13810/j.cnki.issn.1000-7210.2002.04.022

Yin, Y. S., Wu, S. H., Zhang, C. M. et al. (2008). Multi-Point Geostatistics Method Based on Reservoir Skeleton. *Science China (D: Earth Sciences), 38,* 157-164. https://doi.org/10.27643/d.cnki.gsybu.2020.001320

Yin, Y. S., Zhang, C. M., Li, S. H. et al. (2014). A Pattern-Based Multiple Point Geostatistics Method. *Geological Review, 60,* 216-221. https://doi.org/10.16509/j.georeview.2014.01.005

Zhang, R., Sen, M. K., Phan, S., & Srinivasan, S. (2012). Stochastic and Deterministic Seismic Inversion Methods for Thin-Bed Resolution. *Journal of Geophysics and Engineering, 9,* 611-618. https://doi.org/10.1088/1742-2132/9/5/611

Zhou, J. Y., Gui, B. W., & Lin, W. (2010). Application of Multiple-Point Geostatistics in Offshore Reservoir Modeling. *Journal of Southwest Petroleum University (Science & Technology Edition), 32,* 70-74.